

# Simulations of the Nuclear Recoil Head-Tail Signature in Gases Relevant to Directional Dark Matter Searches

P. Majewski<sup>a,\*</sup>, D. Muna<sup>a</sup>, D.P. Snowden-Ifft<sup>b</sup>, N.J.C. Spooner<sup>a</sup>

<sup>a</sup> *Department of Physics and Astronomy, University of Sheffield, S3 7RH, UK*

<sup>b</sup> *Department of Physics, Occidental College, Los Angeles, CA 90041, USA*

---

## Abstract

We present the first detailed simulations of the head-tail effect relevant to directional Dark Matter searches. Investigations of the location of the majority of the ionization charge as being either at the beginning half (tail) or at the end half (head) of the nuclear recoil track were performed for carbon and sulphur recoils in 40 Torr negative ion carbon disulfide and for fluorine recoils in 100 Torr carbon tetrafluoride. The SRIM simulation program was used, together with a purpose-written Monte Carlo generator, to model production of ionizing pairs, diffusion and basic readout geometries relevant to potential real detector scenarios, such as under development for the DRIFT experiment. The results clearly indicate the existence of a head-tail track asymmetry but with a magnitude critically influenced by two competing factors: the nature of the stopping power and details of the range straggling. The former tends to result the tail being greater than the head and the latter the reverse.

*Key words:* Dark matter, Directional detector, Gas detector, WIMP, neutralino, TPC, Simulation

*PACS:* 95.35.+d, 29.40.Cs42, 87.55.Gh

---

## 1 Introduction

Measurement of the direction of a low energy ( $\approx 1$  keV/amu) nuclear recoil track and the ionization charge distribution along it, resulting from the elastic scattering of a target nucleus by an incoming WIMP (Weakly Interacting Massive Particle) provides, an unambiguous identification of WIMPs as responsible for the galactic dark matter [1]. Amongst current radiation detection technologies only Time

---

\*Corresponding author:

*Email address:* pawel.majewski@stfc.ac.uk (P.Majewski)

Projection Chambers filled with low pressure gas, appear capable of such a measurement. This prospect has been demonstrated by the directional Dark Matter search R&D experiments DRIFT [2], NEWAGE [3] and MIMAC [4] using Time Projection Chambers (TPCs) filled with low pressure  $\text{CS}_2$  and  $\text{CF}_4$ . In these detectors attempts are currently made to reconstruct the orientation of the low energy nuclear recoil tracks, typically of a few millimetres in length. However, due to the character of the electronic and nuclear stopping powers of low energy nuclear recoils in gas, an asymmetric ionization charge distribution along their tracks may also be expected. Thus additional information on the absolute direction of recoils might be also available. Such potential information on the track sense is termed the head-tail effect, for instance describing the location of the majority of the ionization charge as being either at the beginning half (tail) or at the end half (head) of the track. It is known that if this information can clearly be extracted in a detector this would, by breaking the forward-back degeneracy in the direction of recoils from WIMPs, have a dramatic impact on the potential directional sensitivity to dark matter, an effect likely to be of order  $\times 10$  or more [5].

Realisation of this gain would greatly increase the feasibility of building a large dedicated low pressure TPC detector capable of a definitive identification of dark matter. It is thus vital to understand whether, and to what magnitude, the head-tail effect is present, in both principle and practice. Recently some experimental evidence for head-tail asymmetry has been observed for F recoils in 100-380 Torr  $\text{CF}_4$  [6]. Observation of the effect there was possible due to the use of relatively high energy recoils ( $>200$  keV) and a short drift gap. However, measurement of the effect in a more realistic scenario for dark matter searches, in a large volume (order  $\text{m}^3$ ), with negative ion gas and at lower recoil energy, is more difficult. This is due to the limited spatial resolution imposed by the current readout technologies used for larger scale detectors, for instance Multiwire Proportional Counters (MWPCs) as in DRIFT, and due to the inevitable effects of ionization charge diffusion in large detectors. Only preliminary experimental measurements have been possible so far with DRIFT itself [7]. Thus, in view of the importance of the issue for directional dark matter detection, the need to understand better the physical processes so as to help optimise implementation of possible head-tail discrimination in a large detector, it is useful to undertake detailed simulations of the head-tail response and start to make theoretical predictions. This is the objective of the work presented here. In this light it should be noted that the purpose here is not to detail a complete head-tail simulation for a specific detector such as DRIFT II (the subject of a separate paper) but to explore the issue in a more generic fashion.

So far some basic theoretical predictions of the head-tail effect in binary gases have been performed by A. Hitachi, i.e. [8]. These results were based on the Linear Energy Transfer calculations and ion projected range estimations from SRIM [9]. The obtained Bragg-like curves indicated that more ionisation charge is produced at the tail than at the head of the track, regardless of the ion type or energy. However, that work did not attempt to account for straggling, or address the issue of diffusion and the influence of track reconstruction geometry. In this work we present first detailed results of simulations of the energy loss and ionization charge distribution

along tracks of carbon and sulfur ions in 40 Torr CS<sub>2</sub> ( $\rho=1.67 \cdot 10^{-4} \text{ gcm}^{-3}$ ) and for fluorine ions in 100 Torr CF<sub>4</sub> ( $\rho=4.73 \cdot 10^{-4} \text{ gcm}^{-3}$ ). The head-tail effect is studied as a function of ion energy and diffusion but also in relation to the effect of straggling and the dependence on readout geometry.

## 2 Simulation procedures and SRIM results

The basis of this work is firstly the SRIM (Stopping and Range of Ions in Matter) software package and its incorporated TRIM track generator Monte Carlo program. SRIM is a code commonly, and primarily, used for predictions of parameters relevant to ion implantation, sputtering and transportation in solid materials. However, it is also successfully used to simulate interactions in gases, though for that application there has been less experimental verification so that some caution is needed, particularly at the low pressures relevant to this work. SRIM is used here to produce tables as a function of energy of both the electronic ( $S_e$ ) and nuclear ( $S_n$ ) energy loss, stopping power, range, longitudinal and lateral straggling of nuclear recoils (ions) in the gaseous target chosen. The TRIM component is then used to generate many individual simulated tracks. This allows initial investigation of the energy loss distribution along individual raw recoil ion tracks and their secondaries, on an event-by-event basis. To complete the process, to give relevance to real detector scenarios, it is then necessary to convert, using the known average energy to create electron-ion pairs (W-value), the energy loss along each recoil track into ionization charges, or number of Negative Ion Pairs (NIPs), distributed along the track. Finally, it is necessary to account for the effects of diffusion of the tracks through a realistic drift volume (taken here to be up to 50 cm) and of the effects of projection onto readout axes. An in-house Monte Carlo was written for these latter stages, with appropriate values for the W to NIPs conversion factor, changing as a function of ion energy.

In this work we calculate parameters for the selected recoil ions using energies up to 500 keV. Fig. 1 and Fig. 2 show SRIM results for the energy loss, lateral and longitudinal straggling, plotted against recoil ion range for ion energies selected at 50 keV intervals. As can be seen in these figures, at higher energies the electronic energy loss is dominant and decreases with energy, whereas at lower values the nuclear energy loss becomes greater than the electronic and increases with decreasing energy, at least initially. For example, for sulphur ions the nuclear energy loss starts to dominate at 100 keV. This means that the energy loss along the ion track is not continuously decreasing, as might naively be expected.

The amount of energy loss due to nuclear interactions as a function of ion energy is presented in Fig 3. The difference in nuclear energy loss between the different ions is clearly seen here. For carbon ions 50% or more of the total energy is lost via nuclear interactions for energies  $E < 20$  keV, whereas in fluorine and sulphur the equivalent factor occurs at much higher energy, 90 and 200 keV, respectively. This energy loss produces very low energy nuclear recoils which can produce significant ionization.

Due to continuous collisions with gas atoms the direction of moving ions also

deviates from their original path. This causes fluctuations in the recoil ions range described by the lateral and longitudinal straggling as a function of ion energy. This parameter, divided by the range, is shown in Fig 2. Here one can see that as the ions slow down they experience increasing straggling relative to the drift length they have ahead, rising sharply at the very end of the track.

Tables of parameters such as those above, calculated using SRIM, are used in the Monte Carlo generator component of SRIM called TRIM to generate tracks. In addition to on-line histogramming of various quantities, TRIM results are also recorded event by event in two different formats. The first is included in the file called *COLLISON.TXT*, generated either in quick simulation mode or as a full nuclear recoil cascade simulation. For the former mode the current energy, position in 3D and type of secondary recoils with their initial energy is recorded for every ion collision. For the latter, information about the energies and positions of all created nuclear recoils is added. TRIM also creates an output file called *EXYZ* which delivers information on the primary ion electronic and nuclear energy loss along the track with high spatial resolution. This format was chosen here for analysis of the head-tail effect.

On this basis, for each recoil ion with a given energy,  $10^4$  events were generated, recorded and further analysed. The energies used were for fluorine: from 100 to 400 with a step of 50 keV; sulphur: from 10 to 100 with a step of 10 keV then up to 250 with a step of 25 keV and up to 400 with a step of 50 keV and carbon from 10 to 100 with a step of 10 keV then up to 200 keV with a step of 25 keV and up to 300 with a step of 50 keV. Each track event in the TRIM output *EXYZ* file contained on average 100 collision points with information on the current ion energy, the 3D coordinate of the collision point and the electronic energy loss.

In order to generate the number of electron-ion pairs, produced along a recoil track it is essential to know the W-value and its dependence on ion energy. In this way, for each ion of a given energy, an appropriate W-value can be selected at every collision point according to its current energy.

For carbon and sulphur ions W-values were selected using the data shown in Fig. 4. Here two sets of values are presented, the first set are measured values taken from [10] and the second are predicted values derived by A.Hitachi [11]. As seen in Fig. 4 there is only partial agreement between published data and simulation. Furthermore, in both cases the value of W at energy below 20 keV is not well determined. For the purposes of this work, as shown in Fig. 4, it was decided to use primarily the experimental data and to use a fit function in the form of:  $f(x) = a + \frac{b}{x^c}$  where a, b and c are free parameters, to the data points, including an extrapolation below 20 keV. Values of the fit parameters used in this work are shown in Table 2.

Using the W-value fit of Fig. 4, the ionisation energy loss and ionisation charge spatial distributions, and hence head-tail effects, were studied for two different geometric configurations relative to the ion interactions points: (i) along the track, and (ii) projected onto an axis aligned with the initial direction of the ion. These geometries allow exploration of the influence of readout on head-tail sensitivity. In particular, first configuration represents the ideal case of perfect 3D track reconstruction. The second configuration is relevant to a simpler 1D type readout. Fig. 5

shows an illustrative plot with projected lines for readout geometries for an example 100 keV sulphur ion track. On this plot the small circles along the track represent interaction points of energy loss with the size being proportional to the magnitude of the energy loss. It is important to consider that different range straggling will occur for ions of the same energy. Hence, for comparison purposes in this plot and elsewhere, the position of each interaction projected point has been normalised to the projected range of the ion.

### 2.1 Ion Ranges

Based on the processes described above a study was performed first to compare ion ranges, before diffusion, as a function of energy and NIPs. Fig. 6 shows results for sulphur and carbon in CS<sub>2</sub> vs. energy in comparison with data from [10]. Here, the projected range was used, calculated using the coordinates of the first and last point of the ion track. It can be seen that there is a very good agreement for sulphur. For carbon ions however, agreement is less compelling, the results from this work yielding less than half the values in [10]. This discrepancy, which is the subject of further experimental study, although significant does not effect the general conclusions of this work, since sulphur and fluorine have the dominant response for dark matter scattering. For the conversion of the energy loss into ionization charge, the number of electrons attached, with no loss, to CS<sub>2</sub> molecules creating CS<sub>2</sub><sup>-</sup> was summed for each carbon and sulphur ion energy. Fig. 7 shows, as a function of NIPs, the resulting range of nuclear recoils together with the range of alpha particles and electrons calculated with TRIM and ESTAR [12], respectively. The NIP values were calculated here for the latter species using a W-value of 19 eV [13]. It can be seen from Fig. 7, comparing electron recoils with nuclear recoils yielding the same number of NIPs, that the difference in range is typically one order of magnitude greater for electrons than for nuclear recoils. This illustrates the expected great electron (gamma) rejection power of a TPC operating with 40 Torr CS<sub>2</sub>, as has been experimentally confirmed [14]. However, it also shows that the range of nuclear recoils and alpha particles of similar low energy are close to each other, the difference being not greater than 1-2 millimeters for tracks a few millimetres long.

To check further the consistency of the SRIM procedure used here, and developed for the head-tail analysis below, some comparisons was made with existing measurements. In particular, the ranges of 103 keV <sup>206</sup>Pb recoils in several pure and binary gases at STP were calculated and compared with data from [15]. The results are shown in Table 1. As can be seen in most cases there is less than a 10% difference. Similar differences between measurements and simulation were observed for long range 5-6 MeV alpha particles from Rn and Po decays in 40 Torr CS<sub>2</sub> [16].

### 2.2 Head-Tail

Along with the event-by-event information on ion energy loss, TRIM also delivers histograms accumulated on-line and shows distributions of average values of several quantities as a function of target depth. With the default initial TRIM settings in

place the target depth is defined by projection onto the axis of the initial direction of ion motion. One of the histograms shows distributions of the average ionization energy loss by the primary ion recoils and secondary recoils separately as a function of target depth. An example of such distributions is shown in Fig. 8 for 1000 sulphur ions with energy of 100 keV. Here one can see the ionization energy loss by the recoil ion, by the secondary recoils produced and by their sum. The latter is compared in Fig. 8 with scaled results derived from analysis of the *EXYZ* TRIM output file. Reassuringly, both show the same form of ionization energy loss vs. target depth, indicating here that more energy is lost at the beginning of the track (tail) than at the end (head).

However, whilst such averaged SRIM plots are applicable for use in, for instance, ion damage calculations, caution is needed in interpreting or using them directly for studying head-tail discrimination in a dark matter detector. This is because the distribution is an average provided as a function of target depth regardless of the ion range that, due to straggling, varies from ion to ion. For the experiments of interest here, recoils are detected on an event-by-event basis with ionization charge distribution created along the track and then projected onto an axis. For this situation, as pursued here, use of the *EXYZ* track generation output file alone is more appropriate.

Based on this, Figs 9-11 show the distributions of total, nuclear and electronic energy loss for sulphur, carbon and fluorine ions along the track and projected onto the initial direction of the ion motion and normalised to its projected range  $R$ . Calculations were performed for ion energies up to 400 keV. As expected from the stopping power shape for both fluorine and carbon ions with high energies, where the electronic energy loss dominates, the total energy loss distribution has mainly a clear negative slope. This indicates greater energy loss at the tail of the track than at the head. However, due to ion straggling at the very end of the track, the energy loss there accumulates in a small volume that, when projected, creates a clearly visible sharp rise at the end of the energy loss distribution. For lower ion energies the slope at the beginning of distributions gets smaller and for energies below 200 keV and 50 keV for fluorine and carbon respectively it becomes flat. Only the sharp end remains, indicating now that more energy is lost at the head of the track than at the tail. For all studied energies of sulphur ions the energy loss distribution remains largely flat but, like the others, ends with a sharp rise. Clearly this distribution for sulphur differs from the one given in Fig. 8. It shows an opposite effect, because now the influence of straggling is properly included and this can dominate over the stopping power characteristic at the head of the track.

Next, converting from energy loss to ionisation (NIPs) charges, the distributions of ionization charge were studied for sulphur and carbon ions in  $\text{CS}_2$ . This was performed for the geometric scenario when ionization is projected onto the axis of the initial ion motion. The charge diffusion in gas was accounted for by redistributing the NIPs in space according to the thermal diffusion formula:  $\sigma = \sqrt{\frac{2k_B T}{e}} \sqrt{\frac{L}{E}}$  where  $k_B$  is Boltzmann constant,  $T$  ambient temperature,  $e$  electron charge,  $E$  drift electric field and  $L$  drift distance. After numerical simplifications the diffusion formula used

was of form:  $\sigma[mm] = 0.72\sqrt{\frac{L[m]}{E[keVcm^{-1}]}}$  for three different drift lengths  $L$ : 0.0, 0.3 and 0.5 m and electric field  $E= 0.58$  kV/cm as used in the DRIFT IIb detector [14].

The head-tail effect information was quantified using the same parameter as formulated for the DRIFT II data analysis described in [7], on an event-by-event basis that is  $Ratio = \frac{\int_0^{50\%R} NIPs}{\int_{50\%R}^{100\%R} NIPs}$  charge integrated along the two halves of the projected range  $R$ . Fig. 12 shows results of the head-tail effect for sulphur and carbon tracks, respectively. Results are given as a function of ion energy for three different W-value data sets described earlier. To illustrate the impact of diffusion for instance as might be expected in an experimental run of DRIFT, results are given for tracks drifted for a random distance up to maximum of 0, 30 and 50 cm. Points with Ratio values above 1 are for ion tracks with greater tail than head and those below for ions with the reverse.

Examining these plots it can be seen that again the head-tail effect depends on the ion energy as expected. The effect is greatest for carbon at high energies where the tail dominates but reduces towards lower energies, the asymmetry eventually switching to domination by the head below typically 60 keV. For sulphur, the head-tail effect is generally found to be smaller but varies less with recoil ion energy and maintains tail domination for almost all energies.

This is expected since with this geometry the effect of the straggling is extracted more accurately. Finally, it can be seen that there is some dependence of the head-tail effect on the W-value used. The increased values at low energy from the Hitachi et al. prediction result in further enhancement of the head-tail asymmetry.

### 3 Conclusions

In this work preliminary results of the head-tail effect of carbon and sulphur ions in low pressure  $CS_2$  gas as used in DRIFT detectors have been presented. Results were obtained using the SRIM/TRIM package with a purpose-written Monte-Carlo and W-values available from both existing and theoretical data. The shape of the ionisation charge distribution along an ion track, without effect from ion range straggling, is found to be similar to that previously presented by Hitachi. It shows that for ion energies down to 10 keV more ionization charge is created at the tail than at the head, irrespective of the ion type. However, when full account is taken of straggling at the end of tracks and diffusion, particularly in relation to the geometry of the readout, the situation dramatically changes. For instance, for tracks projected onto the direction of the initial ion motion, results indicate the existence of a head-tail effect with a greater head for energies below 70 and 350 keV for carbon and sulphur respectively. Above these energies the tail starts to dominate. It is further found that the head-tail effect depends on the W-value, values for which below 20 keV are particularly uncertain.

In summary, we note two main conclusions from these initial detailed simulations. Firstly, that for all the scenarios explored here some form of head-tail asymmetry in the low energy ion recoil tracks is expected. Secondly, that the nature of this

asymmetry, including the sense (whether head or tail is dominant), can not be predicted by simple consideration of the average ionisation loss simulations, but rather is critically influenced by details of the straggling, readout used and W-values at low energy. More experimental effort, underway by the DRIFT collaboration and others, is needed to untangle these issues.

#### **4 Acknowledgements**

Authors would like to thank prof. A. Hitachi for valuable comments and sharing his calculation results of the W-values for Sulfur and Carbon ions in CS<sub>2</sub> and prof. J.F. Ziegler for his help in SRIM calculations. P. Majewski would like to thank support given through University of Sheffield contract DF7016 and ILIAS contract RII3-CT-2004-506222.



## References

- [1] J.D.Lewin and P.F.Smith, *Astroparticle Physics* **6** (1996) 67
- [2] S. Burgos et al., *Nucl. Instr. Meth. A* **584** (2008) 114
- [3] K. Miuchi et al., *Physics Letters B* **654** (2007) 58
- [4] E. Moulin, M. Mayet and D. Santos, *Physics Letters B* **614** (2005) 143
- [5] B. Morgan, A. M. Green and N. J. C Spooner, *Phys. Rev D* **71** (1005) 103507.
- [6] D. Dujmic et al., *Nucl. Instr. Meth. A* **584**,327 (2008)
- [7] S. Burgos et al., arXiv:0807.3969
- [8] A. Hitachi, *A Bragg-like curve for the dark matter searches; binary gases.*  
submitted to Rad. Phys. Chem. special issue on ASR2007
- [9] J. Ziegler, SRIM 2006, *The Stopping and Range of Ions in Matter.*
- [10] D. P. Snowden-Ifft et al., *Nucl. Instr. Meth. A* **498**, 155 (2003)
- [11] Private communication.
- [12] ESTAR: stopping power and range tables for electrons,  
<http://physics.nist.gov/PhysRefData/Star/Text/ESTAR.html>
- [13] DRIFT collaboration internal report.
- [14] S. Burgos et al., *Astroparticle Physics***28**, 409 (2007)
- [15] G. L. Cano et al., *Phys. Rev.* **169**, 227 (1968)
- [16] S. Burgos et al., *Nucl. Instr. Meth. A* **584**, 114 (2008)

Gas	Measurement [ $\mu\text{m}$ ]	SRIM [ $\mu\text{m}$ ]
Ar	79	73
Xe	44	36
CH <sub>4</sub>	84	95
C <sub>2</sub> H <sub>4</sub>	58	61
Air	83	80
N	80	74

Table 1: Ranges of 103 keV 206 Pb recoils in pure and binary gases at STP measured and calculated with TRIM. Values from measurement are from [15].  $1\sigma$  of the simulated range distributions is 10% of the tabulated mean values for all gases except Xe for which  $1\sigma$  is 15%. Measurement uncertainty is  $\pm 2\mu\text{m}$ .

Data	a	b	c
S (Ifft)	32.13	289.17	0.79
C (Ifft)	28.78	36850.30	3.18
S (Hitachi)	-489.4	580.46	0.02
C (Hitachi)	3.19	73.30	0.26

Table 2: Values of the parameters from the t to experimental and theoretical data of the W-values shown in Fig. 4

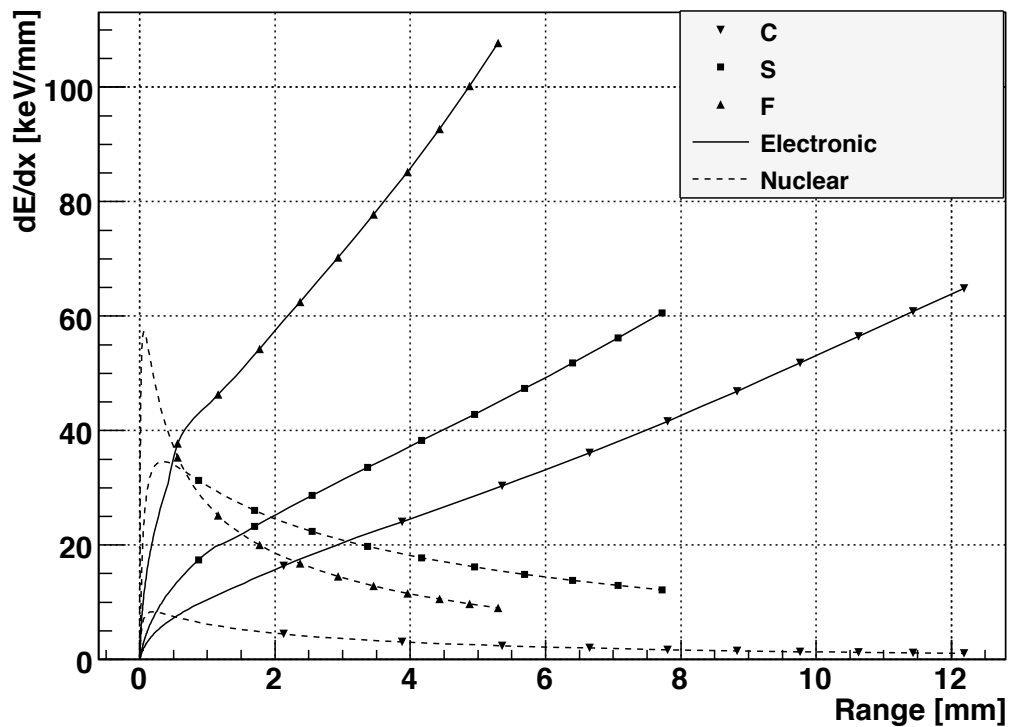


Figure 1: Calculated with SRIM ionization energy loss  $dE/dx$  as a function of ion range in the medium. Energy losses in electronic (solid line) and nuclear (dashed line) channels are shown for Sulfur ( $\blacksquare$ ) and Carbon ( $\blacktriangledown$ ) ions in 40 Torr  $CS_2$  and Fluorine ( $\blacktriangle$ ) in 100 Torr  $CF_4$ . Ion energy is marked up to 500 keV with an interval of 50 keV.

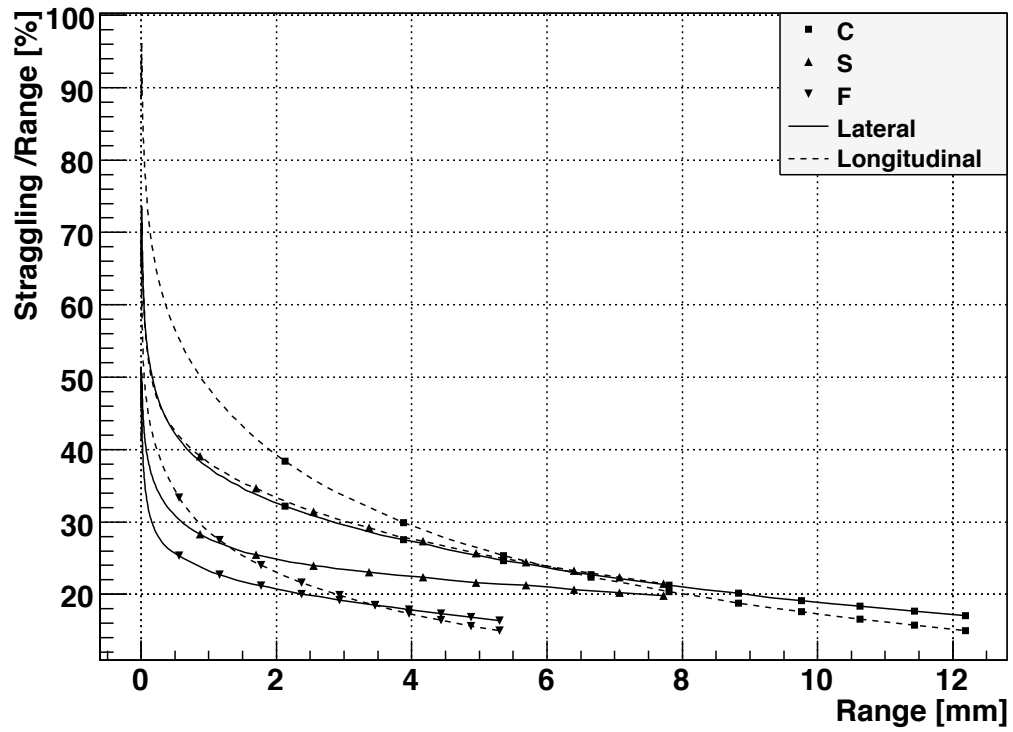


Figure 2: Lateral (solid line) and longitudinal (dashed line) straggling/range as a function of range for Fluorine ions in CF<sub>4</sub> (▼), Sulfur (▲) and Carbon (■) ions in CS<sub>2</sub> which energy is marked up to 500 keV with an interval of 50 keV.

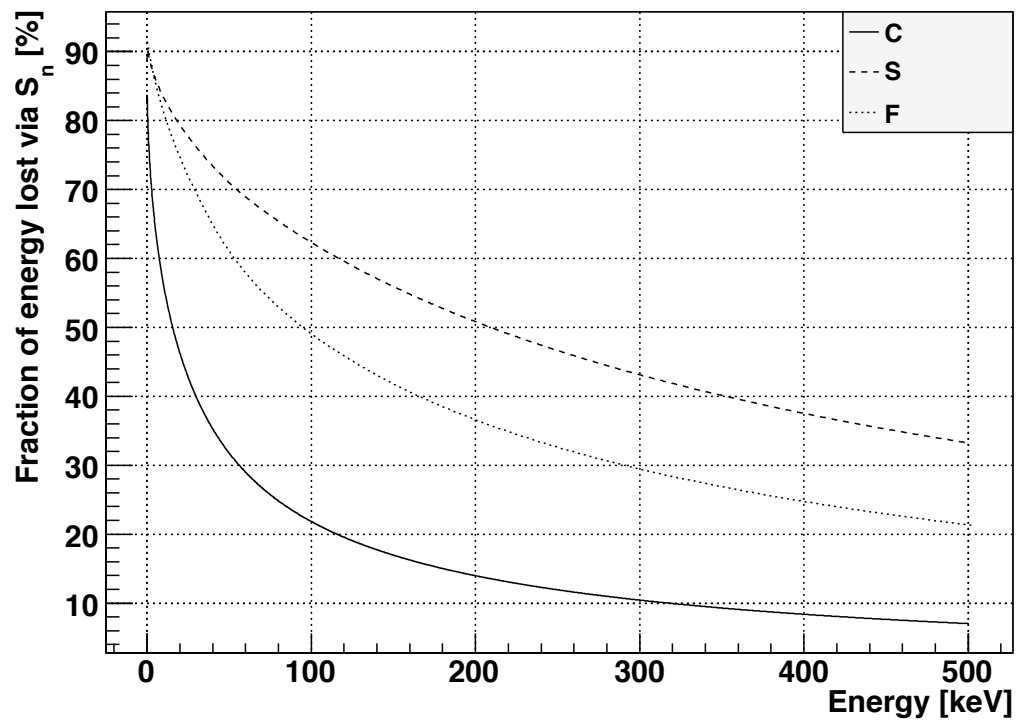


Figure 3: Energy loss due to nuclear interactions with respect to the total energy loss for Carbon, Sulfur in  $CS_2$  and Fluorine ions in  $CF_4$ .

### W-values for C and S recoils in CS<sub>2</sub>

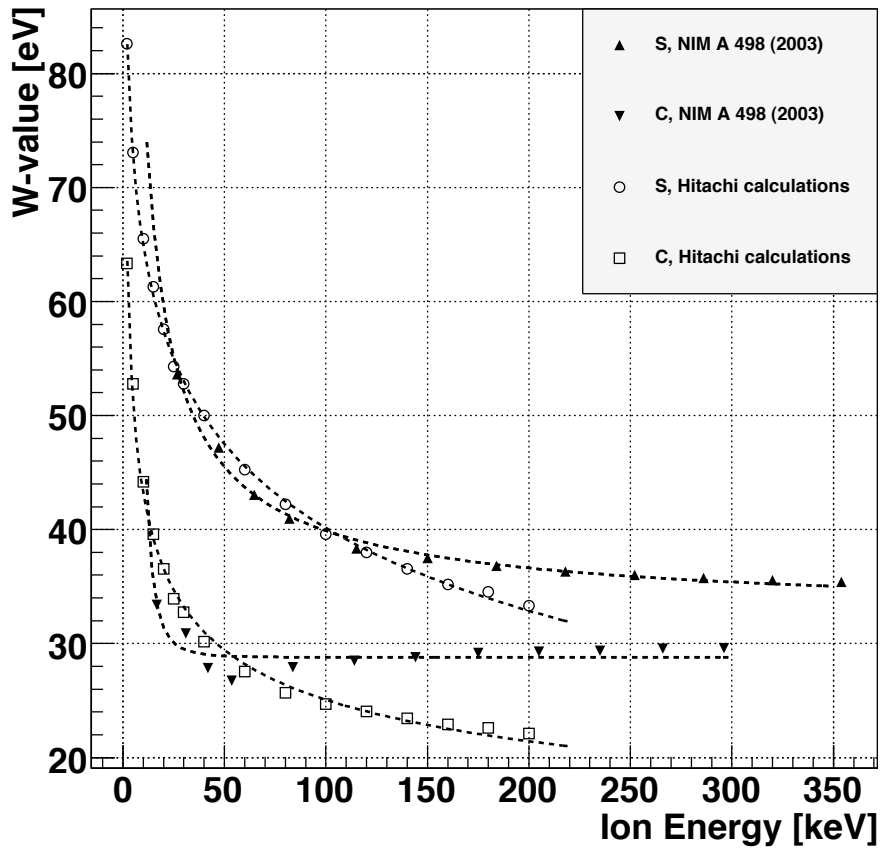


Figure 4: Carbon and Sulfur ions W-values in CS<sub>2</sub> gas as a function of energy. Points marked with ( $\blacktriangle$  and  $\blacktriangledown$ ) show results from [10] while ( $\square$  and  $\circ$ ) values calculated by A. Hitachi. Dashed lines are from a t used for EXYZ TRIM output file analysis.

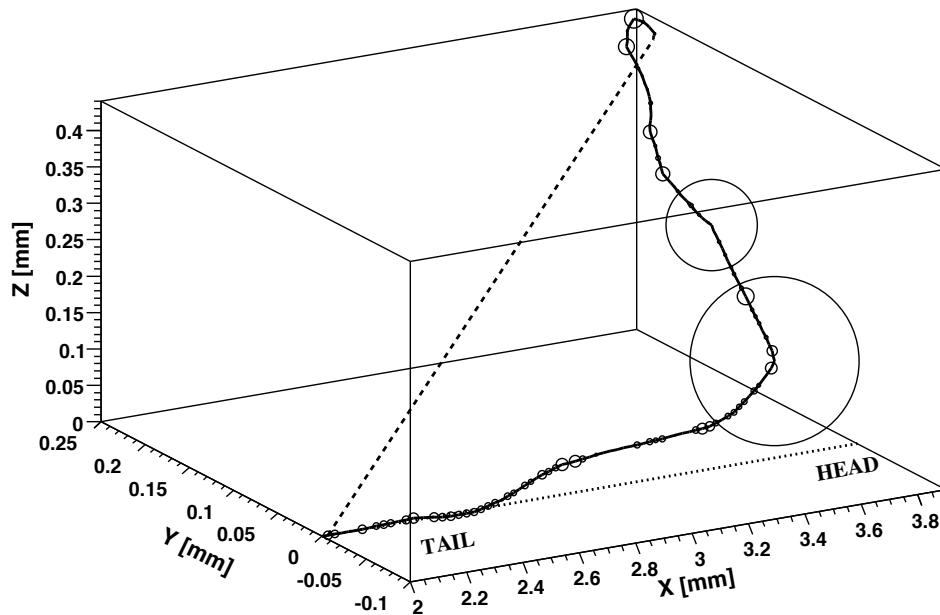


Figure 5: A single track of 100 keV Sulfur ion obtained from *EXYZ* TRIM output. In the work the ionization energy spatial distribution and head-tail effect were studied along: ion track line (solid) and along the axis of the initial motion (dotted). The projected range is denoted by the dashed line. Size of the circles along the track is proportional to the magnitude of the energy loss in the collision. Tail and Head show the position of the beginning and the end of the track, respectively.

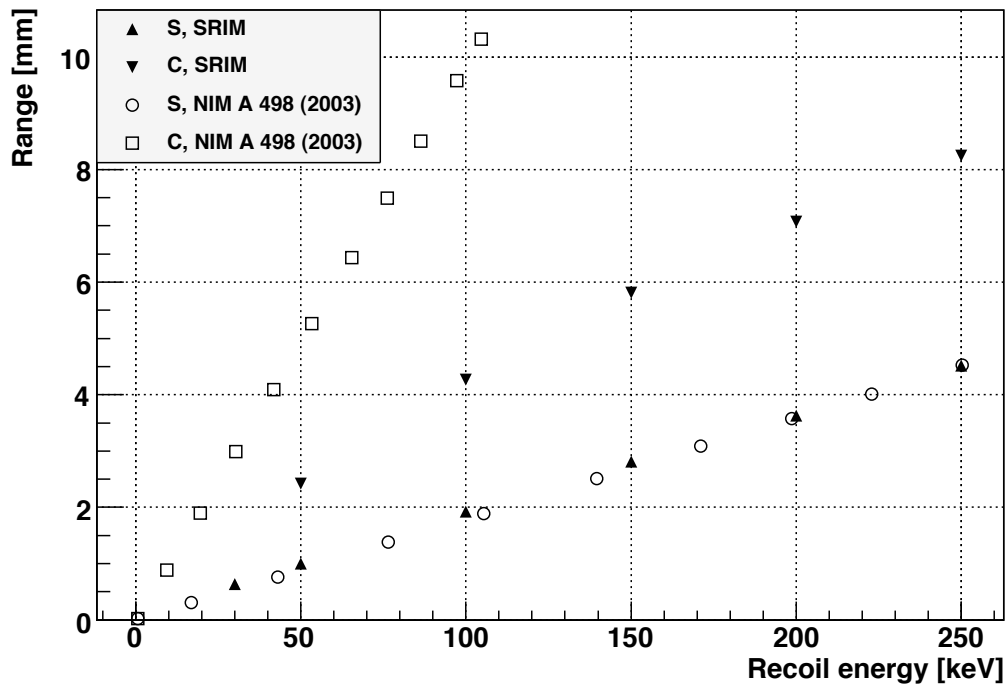


Figure 6: Sulfur and Carbon ion range in  $\text{CS}_2$  as a function of the energy, calculated with SRIM ( $\blacktriangle$  and  $\blacktriangledown$ ) and taken from [10] ( $\circ$  and  $\square$ ).



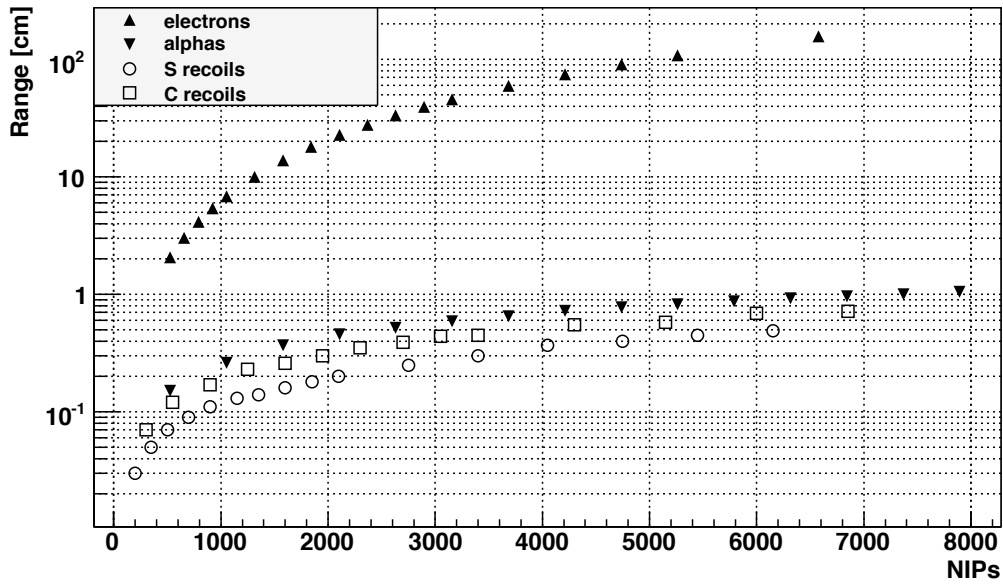


Figure 7: Sulfur ( $\circ$ ), Carbon ( $\square$ ), alpha ( $\blacktriangledown$ ) and electron ( $\blacktriangle$ ) range in  $\text{CS}_2$  as a function of ionization charge (NIPs) created. NIPs for Sulfur and Carbon were calculated using the W-values shown in Fig. 4 while for alpha particles and electrons a constant value of  $W=19$  eV was used. To calculate the range of electrons ESTAR program was used for energies from 10 to 125 keV with steps 2.5, 5 and 10 up to 20, 60 and 100 keV, respectively. Results for alpha particle ranges are for energies from 10 to 150 with a step of 10 keV.

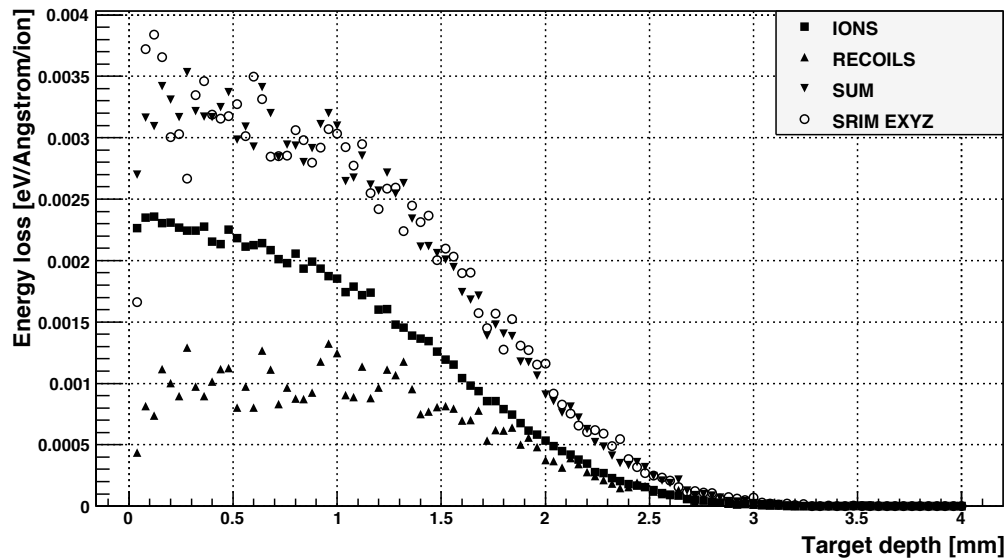


Figure 8: Average ionization energy loss for 100 keV Sulfur ion (■) and created in the cascade secondary Carbon and Sulfur nuclear recoils (▲) as a function of target depth, obtained from TRIM histogramming. Total energy loss (▼) is compared with scaled results from *EXYZ* TRIM output file analysis (○).

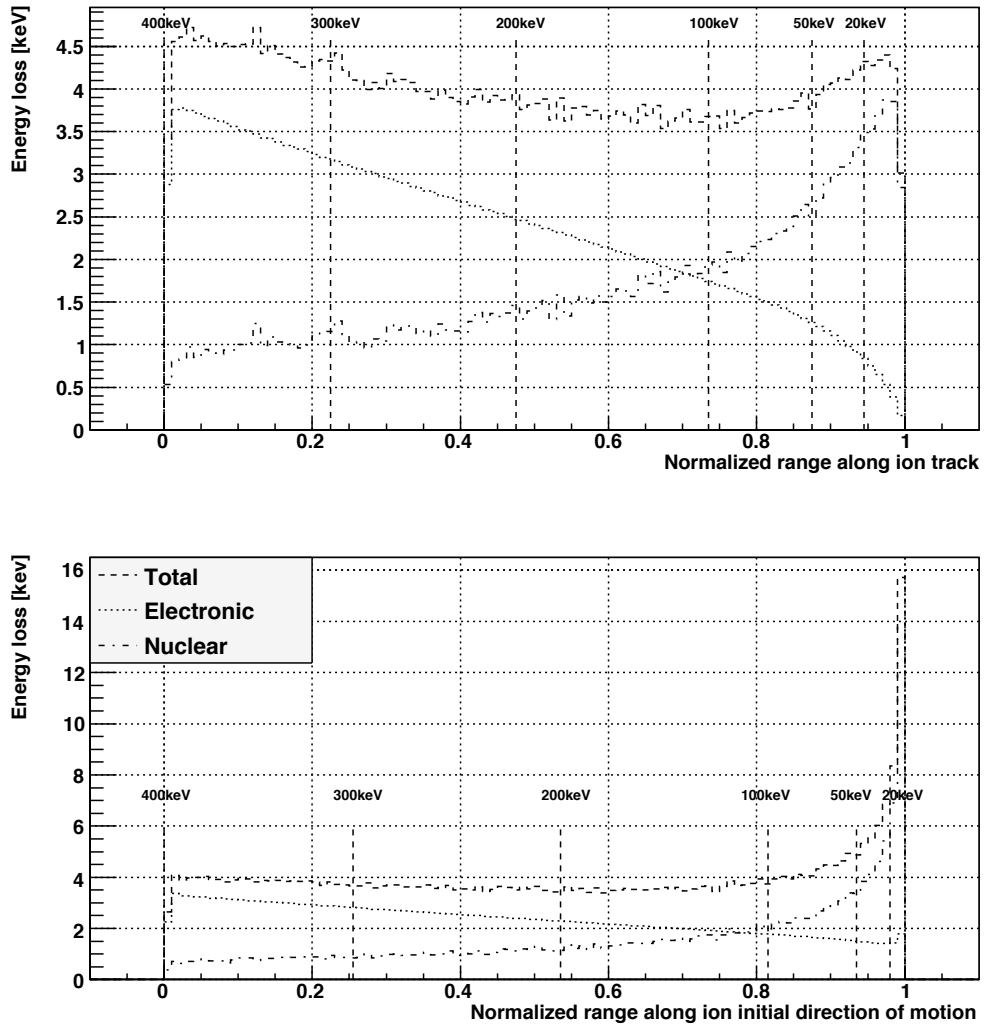


Figure 9: Energy loss distribution for 400 keV Sulfur ion along track (top) and along direction of the initial ion motion (bottom). Dashed, dotted and dash-dotted lines indicate: total, electronic and nuclear energy loss respectively. Vertical dashed lines indicate intermediate ion energy.

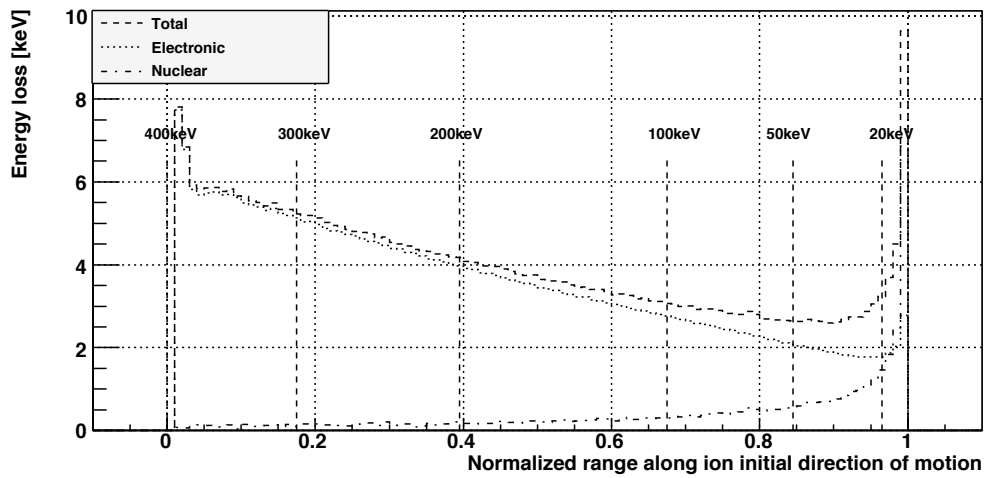
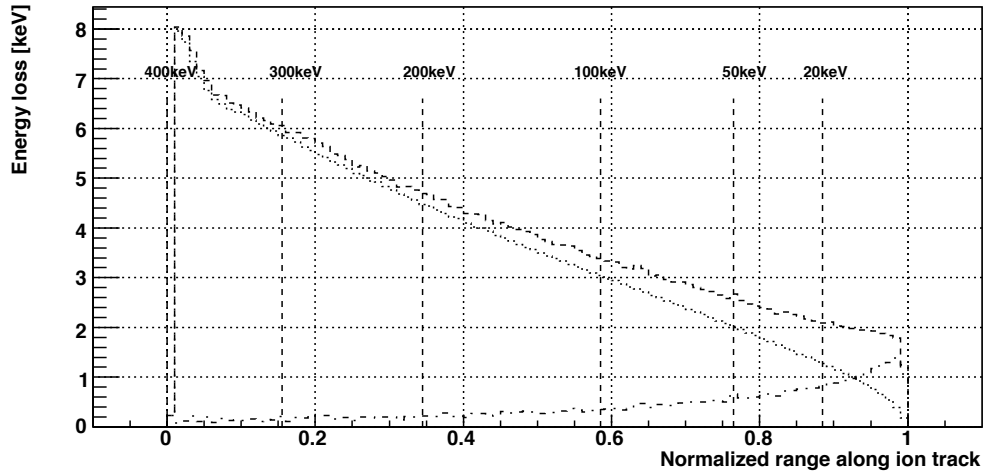


Figure 10: As in Fig. 9 for Carbon ion.

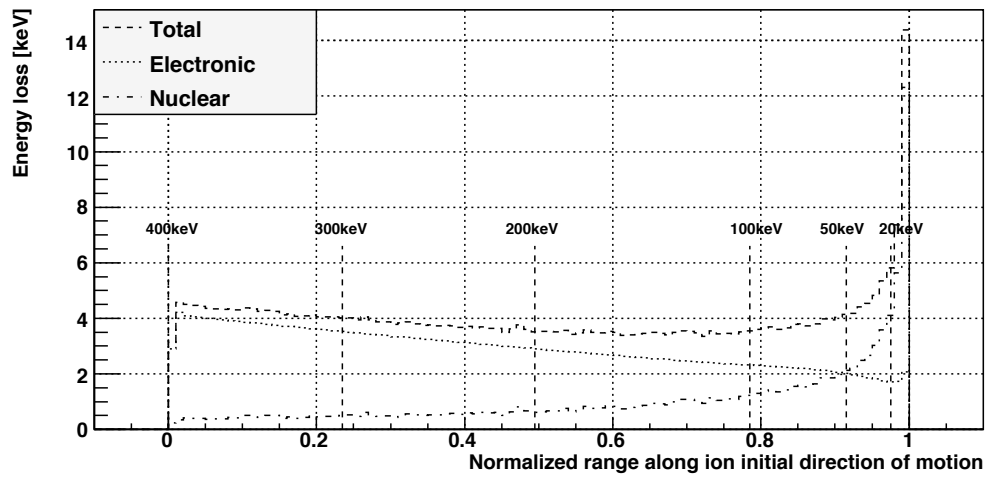
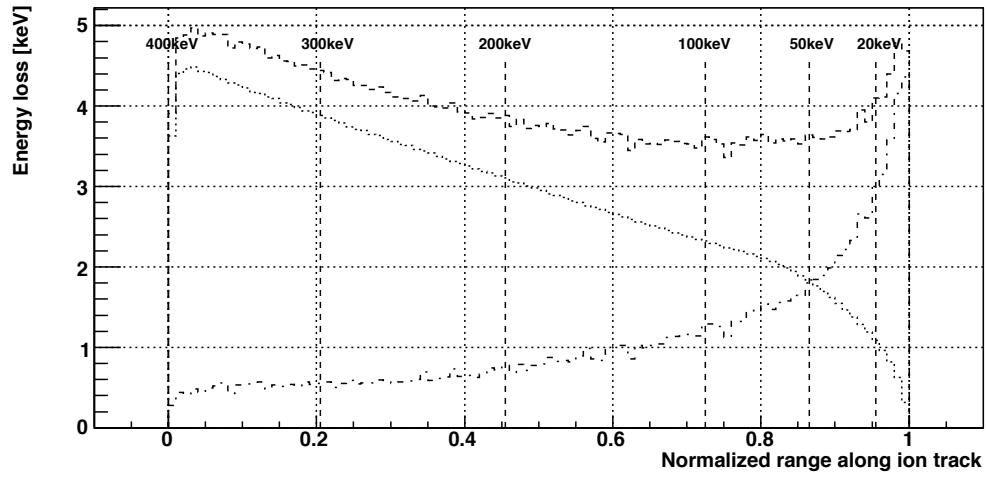


Figure 11: As in Fig. 9 for Fluorine ion.

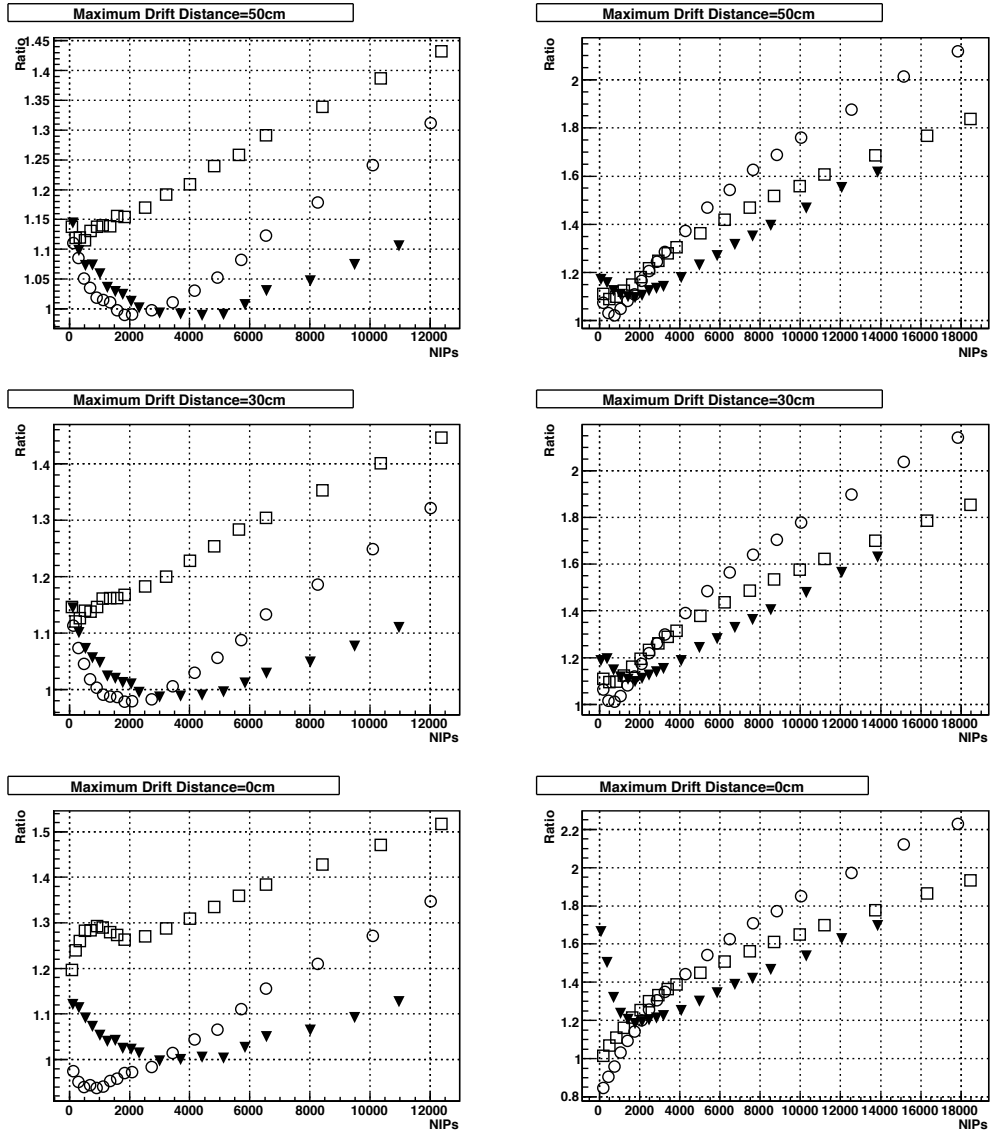


Figure 12: Position of the mean of the charge distribution along Sulfur (left column) and Carbon (right column) ions tracks in  $\text{CS}_2$  showing head-tail effect as a function of energy and maximum drift distance: 50, 30 and 0 cm, for three different W-values: from Hitachi ( $\circ$ ), from Ifft ( $\blacktriangledown$ ) and electronic ( $\square$ ). Points with ratio above 1 indicate that more ionization charge is created at the beginning (tail) while those below that level, at the end (head) of the track.